Top-assisted di-Higgs boson production motivated by baryogenesis

Wei-Shu Hou, Masaya Kohda, and Tanmoy Modak
Department of Physics, National Taiwan University, Taipei 10617, Taiwan

(Received 14 January 2019; published 29 March 2019)

We study top-assisted di-Higgs production via $cg \to tH \to thh$, where h is the 125 GeV scalar boson and H is the CP-even heavy Higgs. The context is the two Higgs doublet model without a Z_2 symmetry, where the extra Yukawa coupling ρ_{tc} generates tH production, with the extra top Yukawa $\rho_{tt} \simeq 0$ to avoid $gg \to H$ constraints. We find that discovery is possible for m_H around 300 GeV or so at the LHC but would need finite $h - H$ mixing angle $\cos\gamma$ to allow for finite λ_{Hhh} coupling, and ρ_{tc} also needs to be not too small. A sizable ρ_{tc} could drive electroweak baryogenesis, which further motivates the search.

DOI: 10.1103/PhysRevD.99.055046

I. INTRODUCTION

The highlight at the LHC so far is the discovery of the 125 GeV scalar boson h [1] in 2012, which resembles rather closely [2] the Higgs boson of the Standard Model (SM). To improve our understanding of the Higgs potential, a key goal at the LHC is to search for di-Higgs, or $pp \to hh$, production. The program is rather challenging, as hh production in the SM [3,4] is rather suppressed. The ATLAS [5–7] and CMS [8–11] experiments have already conducted searches for resonant and nonresonant di-Higgs production, but there is little expectation that the SM process can be observed even at the High-Luminosity LHC (HL-LHC). In this paper, we explore a novel possibility with new physics, that of resonant hh production in association with a top quark.

The context is a two Higgs doublet model (2HDM) with *extra Yukawa couplings*, i.e., without a discrete Z_2 symmetry to impose the Glashow-Weinberg [12] natural flavor conservation (NFC) condition to forbid flavor-changing neutral Higgs (FCNH) couplings. Note that the usual Z_2 symmetry eliminates *all* extra Yukawa couplings. Two processes that feed di-Higgs production can be operative. The existence of extra diagonal Yukawa coupling ρ_{tt} of the exotic CP-even neutral Higgs boson H means that one could have $gg \to H \to hh$ production through a triangle top-quark loop. A second process depends on the FCNH tcH coupling, ρ_{tc}, whereby one can have $cg \to tH \to thh$ (conjugate process implied). In a previous paper [13], we considered turning ρ_{tt} off, so the first process is subdued, and one is left with the second process: di-Higgs and top-associated production. In this paper, we focus on this process, exploiting the extra top quark to investigate possible prospects at the LHC.

We stress that 2HDM without extra Z_2 symmetry could [14] account for baryon asymmetry of the Universe, via electroweak baryogenesis (EWBG). The leading mechanism is via ρ_{tt} and is rather robust. However, in exploring [13] the prospect for a lighter pseudoscalar A boson around 300 GeV, in the face of direct search bounds, we opted to turn off ρ_{tt}, noting that $\rho_{tc} \sim 1$ would still offer an alternative mechanism [14] for EWBG, and hence it is interesting in itself. Thus, the ρ_{tc} driven $cg \to tH \to thh$ process studied here is a companion to the $cg \to tA \to tt\bar{c}$ process that bears a rather intriguing signature.

We find that thh discovery is possible at the HL-LHC for relatively light H, where the associated top quark gives extra handle on background reduction. However, a relatively large Hhh coupling would be needed; hence, the prospect cannot be said to be very likely, but it is not negligible. In the following, we start with the formalism in Sec. II, then continue with the collider signatures in Sec. III, and end with some discussions in Sec. IV.

II. FORMALISM

The CP-even scalars h and H and the CP-odd scalar A couple to fermions by [15,16]

$$-\frac{1}{\sqrt{2}}\sum_{F=U,D,L}\bar{F}_{iL}[(-\lambda^F_{ij}s_\gamma+\rho^F_{ij}c_\gamma)h + (\lambda^F_{ij}c_\gamma+\rho^F_{ij}s_\gamma)H - i\,\mathrm{sgn}(Q_F)\rho^F_{ij}A]F_{jR}+\mathrm{H.c.}, \quad (1)$$

where $i, j = 1, 2, 3$ are generation indices that are summed over and $\lambda^F_{ij} = (\sqrt{2}m^F_i/v)\delta_{ij}$ (with $v \simeq 246$ GeV) and ρ^F are 3×3 real diagonal and complex matrices, respectively. With shorthand $c_\gamma = \cos\gamma$, $s_\gamma = \sin\gamma$, the mixing angle γ is usually written as $\alpha-\beta$ in Type-II 2HDM notation. However, as we advocate no Z_2 symmetry and there exists a second set of Yukawa couplings ρ^F_{ij}, we prefer the notation of Ref. [17], since $\tan\beta$ is ill defined. The FCNH couplings of interest for tcH are $\rho^U_{23}\equiv\rho_{ct}$ and $\rho^U_{32}\equiv\rho_{tc}$. B physics sets stringent limits on ρ_{ct} [16], while ρ_{tc} is only mildly constrained [18], depending on m_{H^+}. In our study, we set $\rho_{ct}=0$ and take $|\rho_{tc}|<1$.

The most general CP-conserving two Higgs doublet potential is given in the Higgs basis as [15,17]

$$\begin{aligned}V(\Phi,\Phi')=&\mu^2_{11}|\Phi|^2+\mu^2_{22}|\Phi'|^2-(\mu^2_{12}\Phi^\dagger\Phi'+\text{H.c.})\\&+\frac{\eta_1}{2}|\Phi|^4+\frac{\eta_2}{2}|\Phi'|^4+\eta_3|\Phi|^2|\Phi'|^2+\eta_4|\Phi^\dagger\Phi'|^2\\&+\left[\frac{\eta_5}{2}(\Phi^\dagger\Phi')^2+(\eta_6|\Phi|^2+\eta_7|\Phi'|^2)\Phi^\dagger\Phi'+\text{H.c.}\right],\end{aligned}\tag{2}$$

where v arises from the doublet Φ via $\mu^2_{11}=-\frac{1}{2}\eta_1 v^2$, while $\langle\Phi'\rangle=0$ (hence, $\mu^2_{22}>0$), and η_is are quartic couplings, again in the notation of Ref. [17]. A second minimization condition, $\mu^2_{12}=\frac{1}{2}\eta_6 v^2$, removes μ^2_{12} and reduces the total number of parameters to nine [17]. The mixing angle γ between the CP-even bosons satisfies the relations [17]

$$c^2_\gamma=\frac{\eta_1 v^2-m_h^2}{m_H^2-m_h^2},\qquad \sin 2\gamma=\frac{2\eta_6 v^2}{m_H^2-m_h^2},\tag{3}$$

for which, for c_γ small but not infinitesimal, one has $c_\gamma\simeq|\eta_6|v^2/(m_H^2-m_h^2)$. This is approximate alignment [17]; i.e., small c_γ values can be attained without requiring η_6 to be small. But in the alignment *limit*, $c_\gamma\to 0$, either [17] η_6 has to vanish (and $m_h^2\to\eta_1 v^2$) or else one has decoupling [19], i.e., $m_H^2/v^2\gg 1$.

We are interested in the Hhh coupling, which is the coefficient of the $\lambda_{Hhh}Hh^2$ term derivable from Eq. (2),

$$\begin{aligned}\lambda_{Hhh}=&\frac{v}{2}[3c_\gamma s^2_\gamma\eta_1+c_\gamma(3c^2_\gamma-2)\eta_{345}\\&+3s_\gamma(1-3c^2_\gamma)\eta_6+3s_\gamma c^2_\gamma\eta_7],\end{aligned}\tag{4}$$

with $\eta_{345}=\eta_3+\eta_4+\eta_5$. It reduces further to

$$\lambda_{Hhh}\simeq\frac{c_\gamma}{2}v\left[3\frac{m_H^2}{v^2}-2\eta_{345}+3\,\text{sgn}(s_\gamma)c_\gamma\eta_7+\mathcal{O}(c^2_\gamma)\right],\tag{5}$$

for small c_γ, so $\lambda_{Hhh}\to 0$ as $c_\gamma\to 0$. To enhance $cg\to tH\to thh$, sizable λ_{Hhh} is needed, and $\eta_{345}<0$ may be preferred so the first two terms add up. However, λ_{Hhh} could still be sizable if $2\eta_{345}\gg 3m_H^2/v^2>0$. Either way, a large $|\eta_7|$ with a proper sign for $\eta_7 c_\gamma s_\gamma$ would help.

The quartic couplings η_1, η_{3-6} can be expressed in terms of m_h, m_A, m_H, $m_{H^\pm}$, and μ_{22}, all normalized to v, as well as the mixing angle γ [17],

$$\eta_1=\frac{m_h^2 s_\gamma^2+m_H^2 c_\gamma^2}{v^2},\tag{6}$$

$$\eta_3=\frac{2(m^2_{H^\pm}-\mu^2_{22})}{v^2},\tag{7}$$

$$\eta_4=\frac{m_h^2 c_\gamma^2+m_H^2 s_\gamma^2-2m^2_{H^\pm}+m_A^2}{v^2},\tag{8}$$

$$\eta_5=\frac{m_H^2 s_\gamma^2+m_h^2 c_\gamma^2-m_A^2}{v^2},\tag{9}$$

$$\eta_6=\frac{(m_h^2-m_H^2)(-s_\gamma)c_\gamma}{v^2},\tag{10}$$

but η_2 and η_7 are not related to masses, nor the mixing angle γ. Thus, we take v, γ, m_h, m_A, m_H, $m_{H^\pm}$, μ_{22}, η_2, and η_7 as the phenomenological parameters. To save computation time, we randomly generate these parameters in the following ranges: $\mu_{22}\in[0,700]$ GeV, $m_H\in[250,500]$ GeV, $m_{H^\pm}\in[300,600]$ GeV, $\eta_2\in[0,3]$, $\eta_7\in[-3,3]$, and γ values that satisfy $c_\gamma\in[0,0.2]$, with $m_h=125$ GeV. We choose two different scenarios for m_A. In the main scenario, we generate $m_A\in[250,500]$ GeV, with $m_H<m_A$, $m_{H^\pm}$. In the second scenario, we take $|m_A-m_H|<\delta$, where the choice of δ is discussed later in the section. We explore up to $m_H=500$ GeV because, while λ_{Hhh} and $\mathcal{B}(H\to hh)$ increases with m_H, the discovery potential for $cg\to tH\to thh$ suffers the drop in parton luminosities for heavier m_H.

The dynamical parameters in the Higgs potential, Eq. (2), need to satisfy perturbativity, tree-level unitarity, and positivity conditions, for which we utilize 2HDMC [20]. 2HDMC uses the input parameters [20] $m_{H^\pm}$ and Λ_{1-7} in the Higgs basis and with v implicit. We identify Λ_{1-7} with η_{1-7}. Further, we conservatively demand all $|\eta_i|\le 3$, while $\eta_2>0$ is required by the potential positivity, in addition to more involved conditions for other couplings. To match the convention of 2HDMC, we take $-\pi/2\le\gamma\le\pi/2$.

We also need to impose the stringent oblique T parameter [21] constraint, which constrains the scalar masses m_H, m_A, and $m_{H^\pm}$ [22,23], and hence η_is. We apply the T parameter constraint [24] on the points that passed 2HDMC, using the expression given in Ref. [23]. The final "scanned points" within 2σ error of the T parameter are plotted in Fig. 1. The upper panel is for $m_H<m_{H^\pm}$, m_A, such that $H\to AZ$, $H^\pm W^\mp$ decays are disallowed, which in turn enhances the $H\to hh$ branching ratio. As expected, the upper range for λ_{Hhh} mildly increases as m_H becomes heavier but vanishes with $c_\gamma\to 0$.

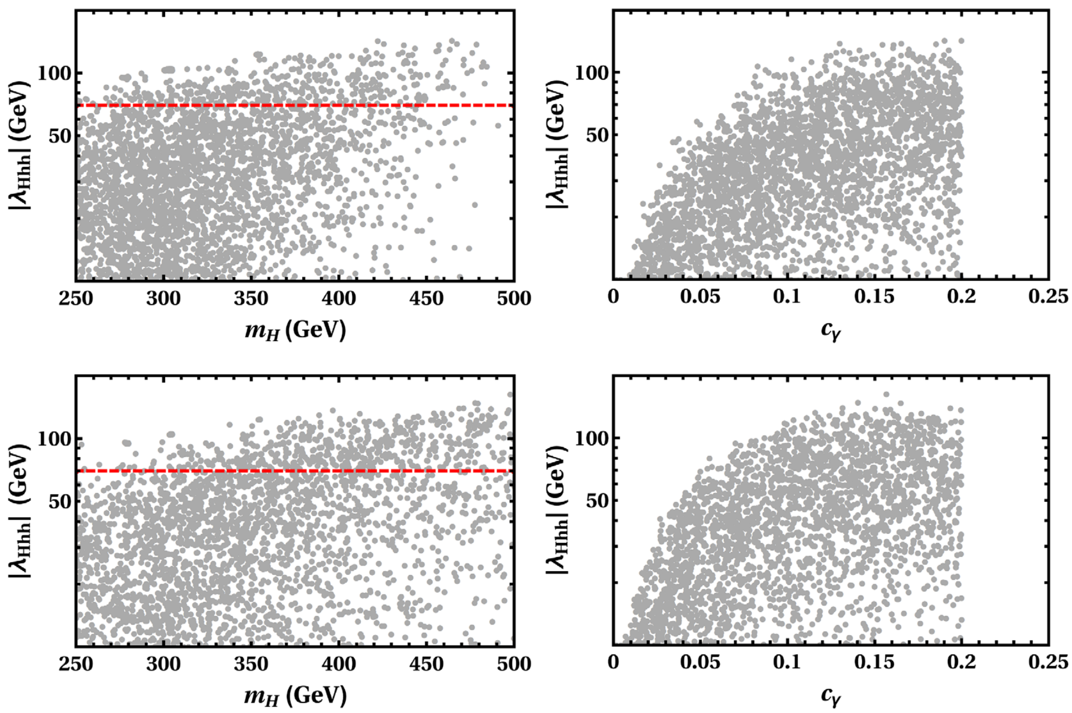

FIG. 1. The λ_{Hhh} vs m_H and c_γ plots for the scan points that pass perturbativity, tree-level unitarity, and positivity through 2HDMC, where $|\eta_i| < 3$ is maintained. The T parameter constraint is also imposed. Upper panels are for $m_H < m_A, m_{H^\pm}$, and lower panels are for $|m_A - m_H| < 5$ GeV. See the text for detailed explanation.

The FCNH coupling ρ_{tc} also receives constraint from CMS four-top search [25] through the $cg \to tH \to tt\bar{c}$ process, which is proportional to $|s_\gamma \rho_{tc}|^2$ [13] if we take $\rho_{ct} = 0$. However, if A and H are mass and width degenerate, the processes $cg \to tA \to tt\bar{c}$ and $cg \to tH \to tt\bar{c}$ cancel each other exactly [13,26], resulting in a potentially much weaker constraint on ρ_{tc}, which can in principle give rise to larger thh production. The lower panels of Fig. 1 are for this scenario of nearly degenerate A and H, where we assume $|m_A - m_H| < \delta$, with $\delta = 5$ GeV for illustration. The dependence of λ_{Hhh} on m_H and c_γ is similar to that in the $m_H < m_{H^\pm}, m_A$ case. We note that in the left panels, i.e., λ_{Hhh} vs m_H, we have drawn a line at $\lambda_{Hhh} \simeq 70$ GeV to illustrate that λ_{Hhh} can be sizable over a finite parameter region.

III. COLLIDER SIGNATURE

The discovery potential of the $cg \to tH \to thh$ (conjugate process implied) depends on the hh decay final states. In this paper, we primarily focus on $t \to b\ell^+\nu_\ell$ ($\ell = e, \mu$) with both h bosons decaying via $h \to b\bar{b}$, giving rise to five b jets, one lepton, and the missing transverse energy (E_T^{miss}) signature. We do not look for hadronic decay of t due to QCD multijet backgrounds, as also discussed in Ref. [27]. In general, $hh \to \gamma\gamma b\bar{b}$ and $hh \to \tau\bar{\tau}b\bar{b}$ modes are suppressed. But $hh \to WW^* b\bar{b}$ decay could provide some sensitivity, which we discuss toward the end of this section.

We set all $\rho_{ij} = 0$ except ρ_{tc} for simplicity throughout this section. Because of the presence of nonzero c_γ, the branching ratios of h will be modified compared to the SM, albeit in a minor way. Since we set all $\rho_{ij} = 0$ except ρ_{tc} and assume $|c_\gamma| < 0.2$, the branching ratios remain practically the same. In the following, we assume all branching ratios of h are SM-like for simplicity.

To illustrate the discovery potential of $cg \to tH \to thh$, we choose six benchmark points (BPs) from Fig. 1 with large $|\lambda_{Hhh}|$ values, which are summarized in Table I. The first three, BP1, BP2, and BP3, are for the $m_H < m_{H^\pm}, m_A$ scenario, while the other three, BPa, BPb, and BPc, are for the $|m_A - m_H| < 5$ GeV scenario. The values of m_H are chosen for $2m_h < m_H < 300$ GeV, $m_H \approx 300$ GeV, and $m_H > 2m_t$ (above the $t\bar{t}$ threshold), respectively. All six benchmark points are for $\eta_{345} < 0$, in accordance with the discussions in the preceding section to achieve large $|\lambda_{Hhh}|$.

The $cg \to tH \to thh$ process depends also on ρ_{tc}. For sizable c_γ, the available parameter space for ρ_{tc} is constrained by the $\mathcal{B}(t \to ch)$ measurement. The latest ATLAS 95% C.L. upper limit (with 13 TeV 36.1 fb^{-1} data) is $\mathcal{B}(t \to ch) < 1.1 \times 10^{-3}$ [28]. Using this limit and our c_γ value, we find the upper limit on $\rho_{tc} = 0.54$, applicable to all six benchmark points. We find the 2σ upper limits on ρ_{tc} for BP1, BP2, and BP3 to be 0.56, 0.55, and 0.63, respectively. The BPa, BPb, and BPc benchmark points were chosen such that the constraint from Ref. [25] becomes much weaker due to cancellation between

TABLE I. Parameter values for the six benchmark points of Table I. See the text for details.

BP	η_1	η_2	η_3	η_4	η_5	η_{345}	η_6	η_7	$m_{H^\pm}$ (GeV)	m_A (GeV)	m_H (GeV)	c_γ	s_γ	$\lvert\lambda_{Hhh}\rvert$ (GeV)	$\frac{\mu_{22}^2}{v^2}$
1	0.287	2.996	−0.188	2.039	−2.555	−0.704	−0.172	0.557	303.27	480.96	279.49	0.169	−0.986	96.80	1.61
2	0.294	2.781	0.269	2.095	−2.945	−0.581	−0.21	0.633	340.18	518.26	303.48	0.169	−0.986	104.32	1.77
3	0.309	2.984	−0.017	2.416	−2.727	−0.328	−0.301	0.881	362.90	536.38	354.15	0.169	−0.986	123.03	2.18
a	0.286	2.97	1.508	−2.189	−0.02	−0.701	−0.169	0.525	377.31	276.72	277.71	0.169	−0.986	96.07	1.59
b	0.294	2.973	1.42	−1.976	−0.037	−0.593	−0.211	0.631	388.90	304.0	303.92	0.169	−0.986	105.06	1.78
c	0.309	2.976	0.294	−0.62	−0.045	−0.371	−0.301	0.932	377.17	353.3	353.89	0.169	−0.986	124.00	2.2

TABLE II. H decay branching ratios for the benchmark points.

BP	ρ_{tc}	tc	hh	WW	ZZ
1	0.54	0.698	0.232	0.049	0.021
2	0.54	0.688	0.238	0.051	0.023
3	0.54	0.677	0.235	0.06	0.027
a	0.54	0.700	0.229	0.049	0.021
b	0.54	0.686	0.240	0.051	0.023
c	0.54	0.674	0.238	0.059	0.027

$cg \to tA \to tt\bar{c}$ and $cg \to tH \to tt\bar{c}$ [13,26]. However, besides the aforementioned $t \to ch$ constraint, ρ_{tc} can still be constrained by $B_{s,d}$ mixing and $\mathcal{B}(B \to X_s\gamma)$, where ρ_{tc} enters via the charm loop through H^+ coupling [16,18]. A reinterpretation of the result from Ref. [18] finds $|\rho_{tc}| \lesssim 1.7$ for $m_{H^\pm} = 500$ GeV [16]. In our analysis, we choose $\rho_{tc} = 0.54$ for all six benchmark points, where the H decay branching ratios are given in Table II.[1]

We remark that the FCNH tuH coupling[2] ρ_{tu} can also induce top-assisted di-Higgs via $ug \to tH \to thh$, and our analysis can be extended to the case in which all $\rho_{ij} = 0$ except ρ_{tu} (see also Ref. [27]). While the ATLAS 95% C.L. upper limit $\mathcal{B}(t \to uh) < 1.2 \times 10^{-3}$ [28] is not much different from the $t \to ch$ case, the CMS four-top search [25] would give a stronger limit on ρ_{tu} than the ρ_{tc} case. The latter is because the relevant process $qg \to tH \to tt\bar{q}$ ($q = u, c$) is enhanced by the parton distribution function (PDF) of the up quark, while the signal region does not differentiate $\bar{u}$ and $\bar{c}$. Similarly and more efficiently, the t-channel scalar exchange process $qq \to tt$ via ρ_{tq} is enhanced by up-quark PDF; hence, the ATLAS same-sign top search [29] may provide a significant constraint in contrast to the ρ_{tc} case [13]. Despite stronger constraints on ρ_{tu}, the discovery potential of $ug \to tH \to thh$ would be balanced to some extent by the similar up-PDF enhancement in comparison to the ρ_{tc} case, but, we do not expect improvement in the signal significance for BP1, BP2, and BP3. By contrast, for an equivalent of BPa, BPb, or BPc, $ug \to tA \to tt\bar{u}$ effectively cancels $ug \to tH \to tt\bar{u}$, relaxing the four-top search limit. The same is true for the ATLAS $qq \to tt$ limit. In such a case, under the $t \to uh$ constraint, ρ_{tu} may be as large as the ρ_{tc} case; hence, we expect a better discovery potential of $ug \to tH \to thh$, boosted by up the PDF.

To investigate the discovery potential of top-assisted di-Higgs production at the LHC, we study $pp \to tH + X \to thh + X$ with both h decaying to $b\bar{b}$, while $t \to b\ell^+\nu_\ell$. The dominant backgrounds are $t\bar{t}$ + jets, single-top, $t\bar{t}h$, $4t$, $t\bar{t}W$, and $t\bar{t}Z$, while tZj, Drell-Yan + jets (DY + jets), W + jets, and tWh are subdominant. We do not include backgrounds from nonprompt and fake sources, as these are not properly modeled in Monte Carlo simulations and require data to estimate. We generate signal and background event samples at leading order (LO), utilizing Monte Carlo event generator MadGraph5_aMC@NLO [30] with default PDF set NN23LO1 [31] for pp collisions at $\sqrt{s} = 14$ TeV, interfaced with PYTHIA6.4 [32] for showering and hadronization, and adopt the MLM matching scheme [33] for matrix element and parton shower merging. The event samples are then fed into Delphes3.4.0 [34] for detector effects (ATLAS based). The effective Lagrangian is implemented using FeynRules2.0 [35].

The $t\bar{t}$ + jets background cross section is normalized to the next-to-next-to-leading-order (NNLO) ones by a factor of 1.84 [36]. The LO Wt component of the single-top cross section is normalized to next-to-leading order (NLO) by a factor of 1.35 [37], while t and s channels are normalized by factors of 1.2 and 1.47, respectively [38]. The $4t$, $t\bar{t}h$, $t\bar{t}W$, and $t\bar{t}Z$ cross sections at LO are adjusted to the NLO ones by factors of 2.04 [30], 1.27 [39], 1.35 [40], and 1.56 [41]. The DY + jets background is normalized to NNLO cross sections by a factor of 1.27 [42,43]. The tWh and W + jets background are kept at LO. The correction factors for conjugate processes are assumed to be the same for simplicity. Note that we do not include the correction factor for the LO signal cross sections.

To distinguish signal from background, we apply the event selection criteria as follows. Each event should contain one lepton and at least five jets, out of which at least four are b tagged (denoted as $4b1\ell$). This reduction in the required number of b jets, from five (one from top decay and four from the h decays) to four [27], is in consideration

[1]Note that for BP3 and BPc the coupling $\lambda_t c_\gamma$ induces $H \to t\bar{t}$ decay. However, for both of the benchmark points $\mathcal{B}(H \to t\bar{t}) \lesssim 0.001$ and are not shown in Table II.

[2]ρ_{ut} is tightly constrained by B_d mixing and $b \to d\gamma$ [18].

TABLE III. Signal and total background (bkg.) cross sections after selection cuts for the $4b1\ell$ process for the benchmark points of Table I, in which the last column gives the significance for 600 (3000) fb^{-1} integrated luminosity.

BP	Signal (fb)	Total bkg. (fb)	Significance 600 (3000) (fb^{-1})
1	0.396	9.002	3.2 (7.2)
2	0.38	9.86	2.9 (6.6)
3	0.288	10.915	2.1 (4.8)
a	0.39	8.906	3.2 (7.1)
b	0.368	9.948	2.8 (6.4)
c	0.295	10.898	2.2 (4.9)

of the finite b-tagging efficiency. The transverse momentum (p_T) of the lepton should be > 28 GeV, while $p_T > 20$ GeV for all five jets. The pseudorapidity (η) of the lepton and all jets should be $|\eta| < 2.5$. We reconstruct jets by the anti-k_T algorithm with radius parameter $R = 0.6$. The minimum separation (ΔR) between any pair of jets, or between the lepton and any jet, should be > 0.4. The E_T^{miss} is required to be greater than 35 GeV.

To reduce backgrounds further, we construct all possible m_{bb} combinations from the four leading b jets and demand that the two m_{bb} pairs that are closest to m_h should lie within 100 GeV $\leq m_{bb} \leq$ 150 GeV. Finally, we demand the invariant mass of the four leading b jets (m_{4b}) to be within $|m_H - m_{4b}| < 100$ GeV. Note that in our exploratory study we have not optimized the m_{4b} cut for each of the benchmark points out of simplicity. We adopt the p_T and η dependent b-tagging efficiency and c- and light-jet misidentification efficiencies of DELPHES. The signal and total background cross sections after selection cuts are summarized in Table III, while individual components of backgrounds are given in Table IV.

We estimate the statistical significance given in Table III by the use of $\mathcal{Z} = \sqrt{2[(S+B)\ln(1+S/B) - S]}$ [44], where S and B are the numbers of signal and background events after selection cuts. We find that, with 600 fb^{-1} data, the significance can reach above approximately 3.2σ for BP1 and BPa, approximately 2.8σ for BP2 and BPb, but only approximately 2σ for BP3 and BPc. With 3000 fb^{-1} at the HL-LHC, the significance can reach beyond 7σ for BP1 and BPa, about 6.5σ for BP2 and BPb, and just below 5σ for BP3 and BPc. The significance depends heavily on the choice of λ_{Hhh} and ρ_{tc}. To get a feeling, we rescaled the significance of the BPs by $\lambda_{Hhh} = 70$ GeV (denoted by red dashed line in Fig. 1) with c_γ and ρ_{tc} fixed as in Table I and Table II, respectively. We find approximately 4.2σ is possible for BP1 and BPa and approximately 3.2σ for BP2 and BPb. The significance is below 2σ for both BP3 and BPc. Note that $\lambda_{Hhh} = 70$ GeV is possible even for lower values of c_γ. A lower c_γ allows larger ρ_{tc} for BPa, BPb, and BPc. Take $c_\gamma = 0.15$ e.g., $\rho_{tc} = 0.61$ (where one can achieve approximately 5σ, 3.8σ, and 2.3σ, respectively, for BPa, BPb, and BPc with 3000 fb^{-1}) is allowed. Though this is not as good as those shown in Table III, it illustrates the chance for finding some signal for lower λ_{Hhh} values, but compensated by gains in ρ_{tc}. BP1, BP2, and BP3 do not have this feature, as discussed earlier. In general, discovery is possible for 270 GeV $\lesssim m_H \lesssim$ 330 GeV with $\lambda_{Hhh} = 70$ GeV for $|m_A - m_H| < 5$ GeV, while the significance drops for the $m_H < m_{H^\pm}, m_A$ scenario. As the parton luminosities falter away, the significance drops rapidly if $m_H \gtrsim 340$ GeV for both scenarios.

Before closing, let us mention briefly the prospect for $pp \to tH \to thh$, where $t \to b\ell^+\nu_\ell$ but one h decays to W^+W^{-*} and the other decays to $b\bar{b}$ (conjugate process implied). Assuming the W and W^* decay leptonically, one has $3b3\ell$ plus the E_T^{miss} (denoted as $3b3\ell$) signature. We find that discovery cannot be attained for any of the six benchmarks at the HL-LHC, but approximately 3.1σ and 3σ are possible for BP1 and BP2, reaching approximately 3σ and 2.9σ significance for BPa and BPb, respectively. The significance for BP3 is 2.5σ, while it is 2.4σ for BPc. Here, we follow the same cut-based analysis as described in Ref. [26] for the $3b3\ell$ process, with the additional requirement of 100 GeV $< m_{bb} <$ 150 GeV. Sensitivity is poor above $m_H \gtrsim 320$ GeV, but if one has nonzero ρ_{tt}, the sensitivity to $cg \to thh$ is lost for $m_H > 2m_t$. This, however, opens up the $cg \to tH \to tt\bar{t}$ triple-top process, which also has $3b3\ell$ signature but without the 100 GeV $< m_{bb} <$ 150 GeV cut, which HL-LHC can actually cover [26]. Indeed, nonzero ρ_{tt} motivates the conventional $gg \to H \to t\bar{t}$ search or $gg \to Ht\bar{t} \to t\bar{t}t\bar{t}$ [45], i.e., the four-top search. The former process suffers from large interference [46] with the overwhelming $gg \to t\bar{t}$ background; however, a recent search by ATLAS found some sensitivity [47]. It

TABLE IV. Cross sections for different background contributions after selection cuts at $\sqrt{s} = 14$ TeV.

BP	$t\bar{t}$ (fb)	Single top (fb)	$t\bar{t}h$ (fb)	$4t$ (fb)	$t\bar{t}W$ (fb)	$t\bar{t}Z$ (fb)	Others (fb)
1	6.701	1.014	1.008	0.016	0.022	0.234	0.007
2	7.418	1.014	1.117	0.019	0.022	0.262	0.008
3	7.939	1.521	1.135	0.024	0.02	0.268	0.008
a	6.616	1.014	1.0	0.016	0.022	0.231	0.007
b	7.425	1.014	1.118	0.019	0.022	0.262	0.008
c	7.923	1.52	1.135	0.024	0.02	0.268	0.008

should be clear, however, that $pp \to tH + X \to thh$ in $3b3\ell$ can provide a supporting role in the top-assisted di-Higgs program at the HL-LHC.

IV. DISCUSSION AND SUMMARY

The 2HDM without NFC allows resonant di-Higgs production via the $cg \to tH \to thh$ process. The process can be searched for at the LHC via $pp \to tH + X \to thh + X$, followed by both h decays to $b\bar{b}$ and $t \to b\ell^+\nu_\ell$. If all other $\rho_{ij} = 0$, this process can be discovered at the HL-LHC in the mass range 270 GeV $\lesssim m_H \lesssim$ 360 GeV if $\rho_{tc} \sim 0.5$ and $\lambda_{Hhh} \sim 100$ GeV. The other decay modes such as $hh \to \gamma\gamma b\bar{b}$, $hh \to \tau\tau b\bar{b}$ are suppressed. Furthermore, $pp \to tH + X \to thh + X$ with $hh \to W^+W^{-*}b\bar{b}$ with $t \to b\ell^+\nu_\ell$ could be sensitive. The significances can be as large as approximately 2σ–3σ depending on the masses of H, A, and $H^\pm$. However, both processes could be preceded by $pp \to tH + X \to tt\bar{c}$, unless H and A are degenerate in mass and width. In such scenarios, nonzero ρ_{tt} helps via $cg \to tH \to tt\bar{t}$ [26]. In general, the presence of other Yukawas reduces the $H \to hh$ branching ratios, making discovery of top-assisted di-Higgs less likely. The cross section for $cg \to tH \to thh$ vanishes as c_γ approaches zero, and the signature requires $c_\gamma \sim 0.15$–0.2. If larger $|\eta_i|$ values are allowed beyond 3, λ_{Hhh} can be enhanced even for smaller c_γ.

Nonzero c_γ would also induce $cg \to tH \to tW^+W^-$ and $cg \to tH \to tZZ$. We find the significances of the former process lie just below 2σ for all the benchmark points with the full HL-LHC dataset. However, for fixed values of c_γ and ρ_{tc}, a smaller λ_{Hhh} enhances the signature for $cg \to tH \to tW^+W^-$ through enhanced $\mathcal{B}(H \to W^+W^-)$. Because of smaller $\mathcal{B}(Z \to \ell\ell)$, we do not find $cg \to tH \to tZZ$ to be promising for any of the benchmark points.

In summary, we have explored associated $tH \to thh$ production at the LHC via $cg \to tH \to thh$, where production involves the extra Yukawa coupling ρ_{tc}, and $H \to hh$ decay needs a finite h–H mixing angle $\cos\gamma \neq 0$ as well as $\mathcal{O}(1)$ extra Higgs quartic couplings. We find a non-negligible discovery potential at HL-LHC for $m_H \sim 300$ GeV. Considering that hh production within the SM is not quite hopeful at the HL-LHC, this is an interesting result. Furthermore, a discovery might shed light on strongly first-order electroweak phase transition. If evidence is found, not only would one have discovered new physics–induced di-Higgs production, but together with the companion same-sign top signal from $cg \to tH \to tt\bar{c}$, one would be probing the ρ_{tc}-driven electroweak baryogenesis scenario provided by this two Higgs doublet model as well as starting to probe the associated Higgs potential.

ACKNOWLEDGMENTS

We thank K.-F. Chen and Y. Chao for fruitful discussions. This research is supported by MOST Grants No. 106-2112-M-002-015-MY3, No. 107-2811-M-002-039, and No. 107-2811-M-002-3069.

[1] G. Aad *et al.* (ATLAS Collaboration), Phys. Lett. B **716**, 1 (2012); S. Chatrchyan *et al.* (CMS Collaboration), Phys. Lett. B **716**, 30 (2012).
[2] G. Aad *et al.* (ATLAS and CMS Collaborations), J. High Energy Phys. 08 (2016) 045.
[3] M. Grazzini, G. Heinrich, S. Jones, S. Kallweit, M. Kerner, J. M. Lindert, and J. Mazzitelli, J. High Energy Phys. 05 (2018) 059.
[4] LHC Higgs Cross Section HH Sub-group, https://twiki.cern.ch/twiki/bin/view/LHCPhysics/LHCHXSWGHH#LHC_Higgs_Cross_Section_HH_Sub_g.
[5] M. Aaboud *et al.* (ATLAS Collaboration), J. High Energy Phys. 01 (2019) 030.
[6] M. Aaboud *et al.* (ATLAS Collaboration), J. High Energy Phys. 11 (2018) 040.
[7] M. Aaboud *et al.* (ATLAS Collaboration), Eur. Phys. J. C **78**, 1007 (2018).
[8] A. M. Sirunyan *et al.* (CMS Collaboration), Phys. Lett. B **778**, 101 (2018).
[9] A. M. Sirunyan *et al.* (CMS Collaboration), J. High Energy Phys. 01 (2018) 054.
[10] A. M. Sirunyan *et al.* (CMS Collaboration), Phys. Lett. B **788**, 7 (2019).
[11] CMS Collaboration, CERN Report No. CMS-PAS-HIG-17-017, 2018.
[12] S. L. Glashow and S. Weinberg, Phys. Rev. D **15**, 1958 (1977).
[13] W.-S. Hou, M. Kohda, and T. Modak, Phys. Lett. B **786**, 212 (2018).
[14] K. Fuyuto, W.-S. Hou, and E. Senaha, Phys. Lett. B **776**, 402 (2018).
[15] See, e.g., S. Davidson and H. E. Haber, Phys. Rev. D **72**, 035004 (2005).
[16] B. Altunkaynak, W.-S. Hou, C. Kao, M. Kohda, and B. McCoy, Phys. Lett. B **751**, 135 (2015).
[17] W.-S. Hou and M. Kikuchi, Eur. Phys. Lett. **123**, 11001 (2018).
[18] A. Crivellin, A. Kokulu, and C. Greub, Phys. Rev. D **87**, 094031 (2013).
[19] J. F. Gunion and H. E. Haber, Phys. Rev. D **67**, 075019 (2003).
[20] D. Eriksson, J. Rathsman, and O. Stal, Comput. Phys. Commun. **181**, 189 (2010).

[21] M. E. Peskin and T. Takeuchi, Phys. Rev. D **46**, 381 (1992).
[22] C. D. Froggatt, R. G. Moorhouse, and I. G. Knowles, Phys. Rev. D **45**, 2471 (1992).
[23] H. E. Haber and O. Stål, Eur. Phys. J. C **75**, 491 (2015).
[24] M. Baak and R. Kogler, arXiv:1306.0571.
[25] A. M. Sirunyan *et al.* (CMS Collaboration), Eur. Phys. J. C **78**, 140 (2018).
[26] M. Kohda, T. Modak, and W.-S. Hou, Phys. Lett. B **776**, 379 (2018).
[27] M. Buschmann, J. Kopp, J. Liu, and X.-P. Wang, J. High Energy Phys. 06 (2016) 149.
[28] M. Aaboud *et al.* (ATLAS Collaboration), arXiv: 1812.11568.
[29] G. Aad *et al.* (ATLAS Collaboration), J. High Energy Phys. 10 (2015) 150.
[30] J. Alwall, R. Frederix, S. Frixione, V. Hirschi, F. Maltoni, O. Mattelaer, H.-S. Shao, T. Stelzer, P. Torrielli, and M. Zaro, J. High Energy Phys. 07 (**2014**) 079.
[31] R. D. Ball, V. Bertone, S. Carrazza, L. Del Debbio, S. Forte, A. Guffanti, N. P. Hartland, and J. Rojo (NNPDF Collaboration), Nucl. Phys. **B877**, 290 (2013).
[32] T. Sjöstrand, S. Mrenna, and P. Skands, J. High Energy Phys. 05 (2006) 026.
[33] J. Alwall *et al.*, Eur. Phys. J. C **53**, 473 (2008).
[34] J. de Favereau, C. Delaere, P. Demin, A. Giammanco, V. Lemaître, A. Mertens, and M. Selvaggi (DELPHES 3 Collaboration), J. High Energy Phys. 02 (2014) 057.
[35] A. Alloul, N. D. Christensen, C. Degrande, C. Duhr, and B. Fuks, Comput. Phys. Commun. **185**, 2250 (2014).
[36] ATLAS-CMS recommended $t\bar{t}$ cross section predictions: https://twiki.cern.ch/twiki/bin/view/LHCPhysics/TtbarNNLO.
[37] N. Kidonakis, Phys. Rev. D **82**, 054018 (2010).
[38] ATLAS-CMS recommended predictions for single-top cross sections using the HATHOR2.1 program: https://twiki.cern.ch/twiki/bin/view/LHCPhysics/SingleTopRefXsec.
[39] SM Higgs production cross sections at $\sqrt{s} = 14$ TeV: https://twiki.cern.ch/twiki/bin/view/LHCPhysics/CERNYellowReportPageAt14TeV2010.
[40] J. M. Campbell and R. K. Ellis, J. High Energy Phys. 07 (2012) 052.
[41] J. Campbell, R. K. Ellis, and R. Röntsch, Phys. Rev. D **87**, 114006 (2013).
[42] Y. Li and F. Petriello, Phys. Rev. D **86**, 094034 (2012).
[43] W.-S. Hou, M. Kohda, and T. Modak, Phys. Rev. D **96**, 015037 (2017).
[44] G. Cowan, K. Cranmer, E. Gross, and O. Vitells, Eur. Phys. J. C **71**, 1554 (2011).
[45] N. Craig, J. Hajer, Y.-Y. Li, T. Liu, and H. Zhang, J. High Energy Phys. 01 (2017) 018.
[46] For a recent reference, see M. Carena and Z. Liu, J. High Energy Phys. 11 (2016) 159, and references therein.
[47] M. Aaboud *et al.* (ATLAS Collaboration), Phys. Rev. Lett. **119**, 191803 (2017).